"Log-Rolling" Alignment in Main-Chain Thermotropic Liquid Crystalline Polymer Melts under Shear: An *In-Situ* WAXS Study

A. Romo-Uribe† and A. H. Windle*

Department of Materials Science and Metallurgy, University of Cambridge, Pembroke Street, Cambridge CB2 3QZ, U.K.

Received February 9, 1996; Revised Manuscript Received June 11, 1996[⊗]

ABSTRACT: This paper sets down in detail the observation, first announced as a note (Romo-Uribe, A.; Windle, A. H. *Macromolecules* **1993**, *26*, 7100), of a strident and reversible orientation transition in a specially synthesized series of thermotropic random copolyester melts of the Vectra A900 type. The transition is between the flow-aligning regime normally seen in nematics and alignment of the global director at right angles to flow-alignment and parallel to the vorticity axis, which we refer to as the "log-rolling" regime. The orientation transition is observed in a comparatively narrow band of temperature above the crystal melting point, the width of this band decreasing with increasing strain rate and increasing molecular weight. We believe that observation of log-rolling in the main-chain thermotropic random copolymers provides confirmatory evidence for the occurrence of a smectic phase in isolated regions which are the precursors of the non periodic layer (npl) crystals which form on further cooling. The fact that the log-rolling regime is not observed at high molecular weights and higher strain rates suggests that the low density of entanglements, which will occur in liquid crystalline polymers with less than completely rigid chains, will nevertheless compromise the log-rolling regime. Slow strain rates and lower molecular weights would each tend to enhance the relaxation of entanglements during shear and thus reduce the deleterious effect which entanglements would have on the log-rolling regime. Recent rheological measurements on the same set of polymers add support to this hypothesis.

Introduction

The importance of liquid crystalline materials derives from the critical roles they play in material and device technologies, as well as in biological systems.[1,2] They are of immediate technological interest not only because of their importance in displays but also by virtue of the extremely strong fibers and films which can be formed from liquid crystalline polymers (LCPs). Thermotropic LCPs are also used for moldings and extrusions, where their good mechanical properties are complemented by excellent mold fill, shape fidelity, and thermal and environmental stability. The microstructures and to some extent the properties of the moldings depend on the processing conditions. The microstructural richness arises from the anisotropy of the local structure, the variety of topological defects that can form in the liquid crystalline phase, and the particular dynamics which give rise to texture evolution under flow.[3−5] However, the prediction of the macroscopic viscoelastic properties of liquid crystalline polymers,[6,7] as well as the state of molecular alignment and the textures produced by flow, remains an important goal.

Microscopic techniques have been developed to detect the formation of complicated morphologies in quenched and sectioned samples subjected to specific thermal and shear flow histories.[8,9] These techniques are unable to follow the development of morphology and microstructure during the shear process, and an important advance has been the development of microscopic experimental techniques which enable *in-situ* flow phenomena studies of polymeric and complex fluids.[3−6,10−19]

This paper presents the results of an *in-situ* WAXS study on main-chain aromatic thermotropic copolyesters, without flexible spacers in the backbone, subjected to steady-shear flow. Measurements have been made using a shearing cell designed for operation in an X-ray generator,[6] which enables the mean orientation with a region defined by the beam (approximately 0.6 mm diameter) to be observed and quantified as a function of imposed shear rate and temperature.

Background

The rheological behavior of untextured lyotropic liquid crystalline polymer systems at modest concentrations is now rather well understood.[7,20−22] Molecular theory[21,22] predicts the two sign changes in the first normal stress difference N_1 as a function of shear rate $\dot{\gamma}$ that have been seen in experiments on lyotropic LCPs.[23−25] These sign changes are associated with a transition from "tumbling" to "wagging" of the molecular director.[22] Wagging is the result of the competition between tumbling and steady alignment of the director along the flow, resulting in oscillations of the director about a steady value. In this wagging regime, the local molecular order is significantly weakened, and N_1 is negative. At high rates of shear, the director aligns well in the flow direction, and N_1 is again positive. In untextured lyotropic nematics, this behavior is now reasonably well understood,[4,5,7,26,27] and in the case of the lyotropic nematic poly(γ-benzyl glutamate), various rheological functions are found to scale as predicted with molecular weight and concentration.[25] Larson and Mead[5] studying flow-induced textures of moderately concentrated lyotropic solutions of poly(γ-benzyl glutamate) (PBLG) mixed with its enantiomorph PBDG reported a sequence of transitions consistent with theoretical predictions based on Doi's rodlike molecular model.

In a general theoretical treatment, Larson and Öttinger[28] have studied the "start-up" problem of simple shearing flow of lyotropic polymeric liquid crystals with the director initially oriented at various angles with respect to the shearing plane (the shearing plane is that containing both the velocity vector $\boldsymbol{v}$ and its gradient $\nabla\boldsymbol{v}$). Their theoretical treatment is important because LCPs are usually textured; *i.e.*, the orientation of the

* To whom correspondence should be addressed.
† Present address: USAF Phillips Laboratory, OL-AC PL/RKFE, 10 E. Saturn Blvd., Edwards Air Force Base, CA 93524-7380.
⊗ Abstract published in *Advance ACS Abstracts,* August 1, 1996.

S0024-9297(96)00211-2 CCC: $12.00 © 1996 American Chemical Society

Table 1. Wholly-Aromatic B−N Copolyesters of 75:25 mol % Composition, with Varying Molecular Weights[a]

	T_m (°C)	
$\bar{M}_w$ (g/mol)	as-received	molded disks
4600	272	273
5000	272	275
8600	274	283
14 400	288	296
30 000	295	295

[a] $\bar{M}_w$ is the weight-average molecular weight, based on viscosity measurements (courtesy of Hoechst-Celanese Corp.). The melting temperatures of the as-received samples and hot-pressed molded disks were measured by DSC.

molecular director varies with position in the sample to give complex microstructural patterns when viewed, for example, in the polarizing light microscope.[3−6] Larson and Öttinger predict a "cascade" of transitions where, at low strain rates, the molecular director will show either tumbling or out-of-plane orientations according to its initial orientation. This out-of-plane orientation corresponds to the maintenance of an initial alignment of the director along the vorticity axis normal to the shear plane ($\boldsymbol{v} \times \nabla\boldsymbol{v}$). Increasing shear rate drives such an out-of-plane director toward the shear plane where it will display "wagging" within the shear plane. Still further increase in shear rate stabilizes the flow, aligning it with the velocity axis.

In a 1993 communication, Romo-Uribe and Windle[29] demonstrated, in main-chain thermotropic copolyesters, the existence of reversible flow-induced orientational transitions between the log-rolling and flow-aligning regimes.[49] Soon afterward, other dynamic scattering studies showed the existence of the log-rolling state in lyotropic polymers and micellar systems.[30−32] Recent investigation on densely packed lyotropic and thermotropic LCPs[33] has shown that their rheological behavior deviates very significantly from Doi's molecular model predictions. In neither case are negative first normal stress differences seen, and scaling behavior in recoverable strain has been observed in only one thermotropic material[34] while scaling in "start-up" experiments is imperfectly followed.[34,35]

Experimental Section

Materials. The research described here focuses on main-chain random copolyesters based on repeat units of 1,4-hydroxybenzoic acid (B) and 2,6-hydroxynaphthoic acid (N), denoted B−N for brevity. The chemical formula is

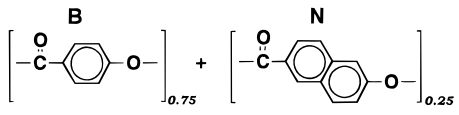

These polymers were specially synthesized by Hoechst-Celanese Corp. in a series of molecular weights. The para-linked ester chain is sufficiently straight and rigid to ensure that the melt phase is liquid crystalline (LC) whereas the random nature of the copolymer reduces the melting point. The polymers were melt synthesized from appropriate ratios of the acetylated monomers, the molecular weight being controlled by terminating the reaction through the metered addition of terephthalic acid. No other additives or catalysts were used. The composition is 75:25 mol % and the weight-average molecular weights $\bar{M}_w$ were determined by Hoechst-Celanese from inherent viscosity measurements in pentafluorophenol/hexafluoro-2-propanol (PFP/HFIP). The molecular weights and crystal melting points are listed in Table 1. These materials have an estimated polydispersity of about 2.[36,37] The crystallinity of the B−N copolyesters at room temperature is of the order of 20% irrespective of molecular weight.[38] The

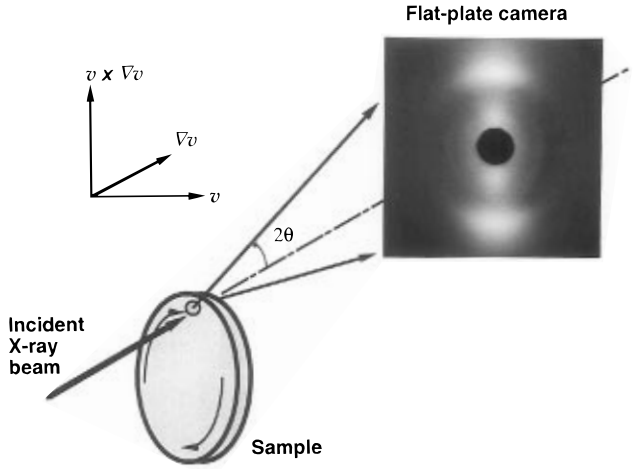

Figure 1. Schematic diagram illustrating the principle of rheo-X-ray scattering experiments. The incident X-ray beam is parallel to the velocity gradient axis ($\nabla\boldsymbol{v}$) and normal to the parallel plates where the sample is held. Due to the design of shear cell geometry, this experiment observes the velocity−vorticity ($\boldsymbol{v}$, $\boldsymbol{v} \times \nabla\boldsymbol{v}$) plane.

B−N copolyesters were received in pellet form and dried under vacuum at 120 °C for 24 h in order to remove moisture. For shear experiments the dried powders were hot-pressed into disks of 25 mm diameter and 1 mm thickness. The molded disks were subsequently stored in a desiccator at room temperature until use (the storage time never exceeded 1 week). The majority of the work described in this paper was carried out on the material of molecular weight 8600 g/mol.

X-ray Shearing Cell. The experiments reported in this work were carried out with an X-ray diffraction shearing cell described in detail elsewhere,[6] and shown schematically in Figure 1. For these experiments, the windows were made of polyimide (Kapton) film 50 μm thick, which permitted an upper working temperature of 340 °C but left no detectable diffraction imprint. The beam diameter was 0.6 mm and exposures were less than 10 min. The film processing was standardized, and the *d*-spacings were calibrated with silicon and quartz powder. Films were digitized and analyzed using SEMPER[39] to give the orientation parameters $\langle P_2 \rangle$, $\langle P_4 \rangle$, etc. Intensities were corrected for empty cell, polarization, geometrical, and absorption factors.

The relationship between the angular velocity ω and the shear rate $\dot{\gamma}$ applied to the specimen at the radial distance of observation r is

$$\dot{\gamma} = \frac{r}{h}\omega \tag{1}$$

where h is the specimen thickness. In the experiments described here, $r \sim 10$ mm and $h \sim 1$ mm: hence $\dot{\gamma} \sim 10\omega$. The experimental protocol was as follows. For shear experiments using fresh molded disks, the temperature was raized at a heating rate of at least 20 °C/min up to the desired temperature in order to prevent any effect of annealing,[38,42] and held for 30 min before shearing to allow temperature equilibrium. Two types of basic experiment were performed: those at fixed shear rate in which the temperature was changed, and those at constant temperature where shear rate was varied. Cu Kα radiation was used throughout, and where patterns were recorded photographically, the specimen−film distance was 4 cm.

Coordinate System. Because of the experimental setup, rheo-X-ray experiments were performed with the incident X-ray beam parallel to the velocity gradient direction as shown in Figure 1. Therefore, the plane imaged on film is that containing the velocity ($\boldsymbol{v}$) and vorticity ($\boldsymbol{v} \times \nabla\boldsymbol{v}$) axes (the velocity direction is tangent to the circular trajectory of the shear cell, and the vorticity axis is along its radius).

Structure of the Polymer before Shear Deformation. The unoriented, as-received HBA-rich copolyester crystallizes as a metastable pseudohexagonal (PH) structure where the main peaks are the prominent 110 equatorial and 211 (Figure

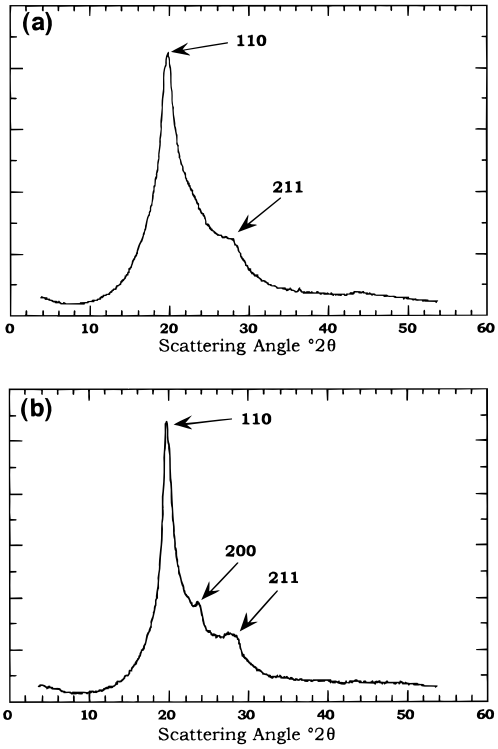

Figure 2. Wide-angle X-ray scattering patterns of B−N 75: 25 mol % $\bar{M}_w$ = 8600 g/mol at room temperature: (a) as-received; (b) hot-pressed molded disk. Diffraction patterns were obtained with a Siemens D500 θ/θ diffractometer in symmetrical reflection mode.

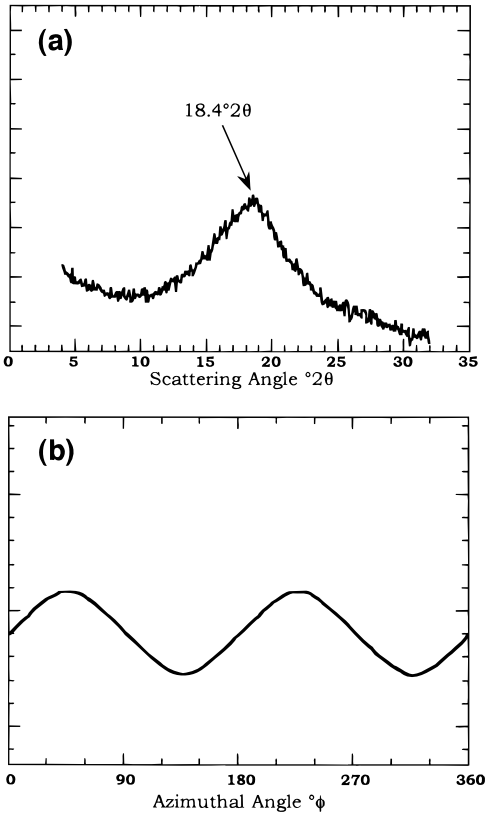

Figure 3. Wide-angle X-ray diffraction traces of B−N 75:25 $\bar{M}_w$ = 8600 g/mol (a) obtained with a position-sensitive detector in the quiescent state at 290 °C before any shear was applied and (b) around the azimuth of the main interchain reflection of the pattern shown in (a).

2a). On annealing, an orthorhombic phase is formed,[38,40−42] characterized by the presence of a 200 equatorial peak in addition to the intense 110. Upon heating the samples to the melt, pressing to form molded disks, and quenching to room temperature, it was found that the copolyesters with $\bar{M}_w \leq$ 14 400 have already transformed to the orthorhombic phase, at least to some extent (Figure 2b). The DSC melting points for the materials formed as disks are compared with the as-received material in Table 1. The increase in melting point for the middle range of molecular weights, while not unexpected, is significant, as it is the higher values which have to be exceeded to obtain a melt sample.

Figure 3 shows a typical X-ray scan of the as-molded 8600 g/mol sample, taken in the shearing cell at 290 °C in the

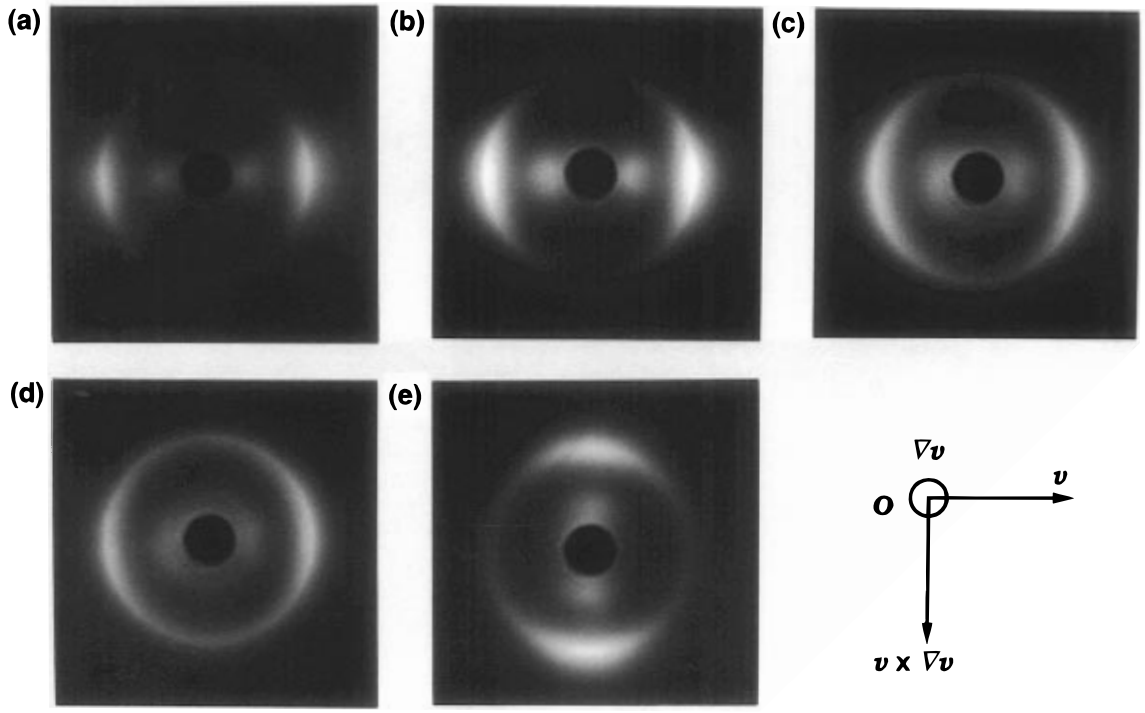

Figure 4. Effect of temperature on the steady-state flow behavior of B−N 75:25 mol % $\bar{M}_w$ = 8600 g/mol while shearing at $\dot{\gamma}$ = 5 s^{-1}. *In-situ* transmission wide-angle X-ray diffraction patterns taken at (a) 285, (b) 290, (c) 295, (d) 300, and (e) 305 °C. In patterns a−c the concentration of equatorial peaks on the velocity axis indicates the orientation of macromolecules along the vorticity axis.

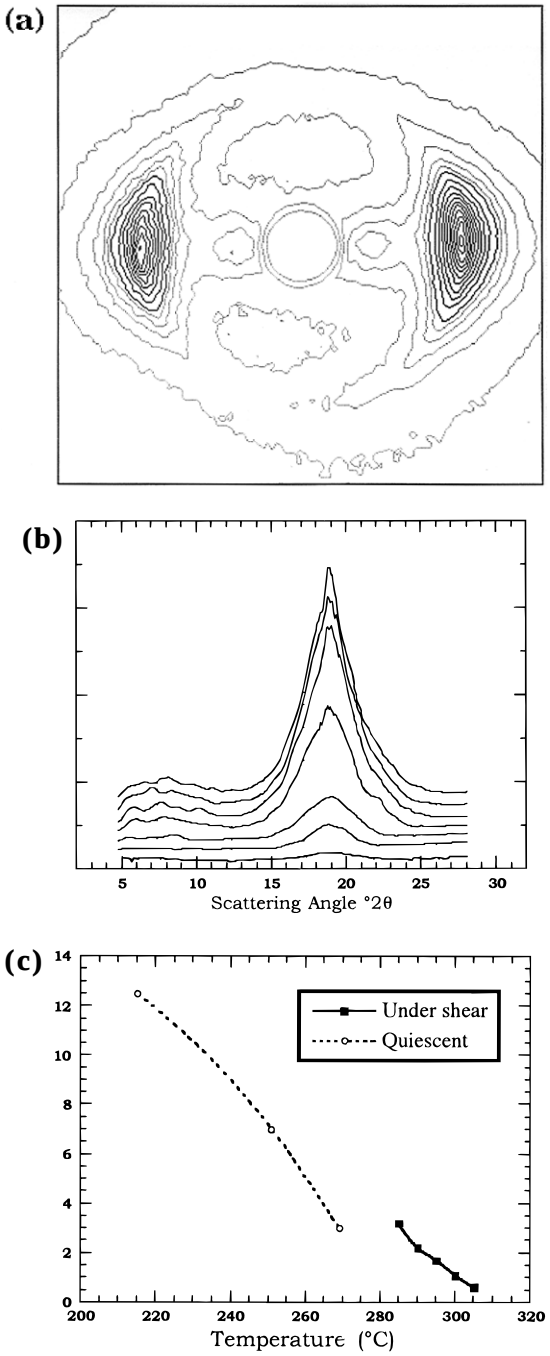

Figure 5. (a) Contour plot of WAXS pattern of B−N 75:25 mol % $\bar{M}_w$ = 8600 g/mol taken at 290 °C while shearing at 5 s^{-1}. (b) Photomicrodensitometer 2θ scans around the azimuth of the pattern shown in (a). Scans were displaced vertically for clarity and correspond from top to bottom to azimuth ϕ = 0°(equatorial), 2°, 5°, 13°, 25°, 35°, and 90° (meridional). The 2θ scans make it possible to separate the small oriented crystalline component which is superimposed on the main liquid crystalline part. (c) Plot of flow-induced crystallinity in the log-rolling regime (filled symbols) and in the quiescent state[36] (open symbols) as a function of temperature.

quiescent state before shear was applied. The intensity pattern has a broad amorphous peak, which indicates that the polymer is fully melted. We also observed, as before,[6] some degree of preferential orientation in the unsheared, quiescent melt, presumably associated with the hot pressing of the sample blank (Figure 3b).

Orientation under Shear

The shear data in this section are all obtained from the 8600 g/mol material.

Effect of Temperature. The effect of temperature on the flow dynamics at a shear rate of 5 s^{-1} was investigated by recording *in-situ* diffraction patterns at different temperatures. Figure 4 shows the results obtained at 285, 290, 295, 300, and 305 °C; the flow direction (***v***) is horizontal in each case, as indicated by the Cartesian axes on the figure. At each temperature, the shear cell was run for a time sufficiently long to ensure that steady-state conditions were attained (at 290 °C and shearing at 5.0 s^{-1}, steady-state conditions were achieved after 3 min). As announced in the previous note,[29] this series shows the striking orientation transition at 305 °C (Figure 4e) between the transverse orientation (the so-called log-rolling regime) shown in Figure 4a−c, where the molecular axes are aligned around the vorticity axis ($\boldsymbol{v} \times \nabla \boldsymbol{v}$) and thus normal to the shear direction, and the flow-aligning regime, where the molecular axes align with the velocity axis. The orientation at 300 °C, which is close to the transition temperature, is not well developed (Figure 4d).

We also note that the diffraction patterns taken at 285 and 290 °C show evidence of very limited crystallinity in the form of a weak, narrow (in 2θ), equatorial arc superimposed on the broad peak characteristic of the liquid crystalline melt. These features, which are only apparent when the polymer is being sheared, are illustrated for 285 °C in Figure 5 a,b, the sequence of peaks corresponding to different azimuthal angles with the nematic liquid crystalline peak being crowned with a sharp crystalline one, while Figure 5c is a plot of crystallinity against temperature under shear at 5 s^{-1}. It is also interesting to note that corresponding orientation coefficients for the two phases are, at 285 °C, $\langle P_2 \rangle_\perp^A = 0.78$ for the amorphous phase and $\langle P_2 \rangle_\perp^K = 0.62$ for the crystalline component. The somewhat poorer orientation of the minority crystalline phase could be taken as indicating that the crystals are not "driving" but, rather, responding to the orientation of the majority melt phase. The shear-induced crystallinity, which has been reported before in flow-aligning Vectra A900,[43] does not prevent stable melt shear being achieved, over periods of the order of several hours at least.

Effect of Shear Rate. Figure 6 shows transmission WAXS patterns of the shearing melt at 290 °C and rates of 0.5, 1.0, 5.0, 10.0, 30.0, and 60.0 s^{-1}; the shear axes are the same as in Figure 4. As before, at each shear rate, the shear cell was run for sufficiently long to ensure that steady-state conditions were achieved. Again, the most striking feature is that at shear rates < 10 s^{-1} log-rolling orientation is apparent, with normal flow alignment at higher strain rates.

Comparison of Figure 6 with Figure 4 for the log-rolling regime shows that the degree of orientation increases with increasing shear rate until the transition is approached, whereas with increasing temperature the decrease is continuous up to the transition. The data are quantified in Figure 7. For convenience, the values of $\langle P_2 \rangle$ for log-rolling are plotted using the negative axes of Figure 7 even though they are, in reality, still positive. The results described above were found to be reproducible, within the experimental error indicated by the error bars in the plots of Figure 7. The flow-induced orientation transitions were independent of direction in which the shear rate was cycled through the transition.

The transitional region was examined at a number of shear rates close to $\dot{\gamma}_c$. Figure 8 shows the diffraction pattern (and its contour plot) right on the transition at 295 °C and $\dot{\gamma}_c \sim 15$ s^{-1}. Note that in this particular case

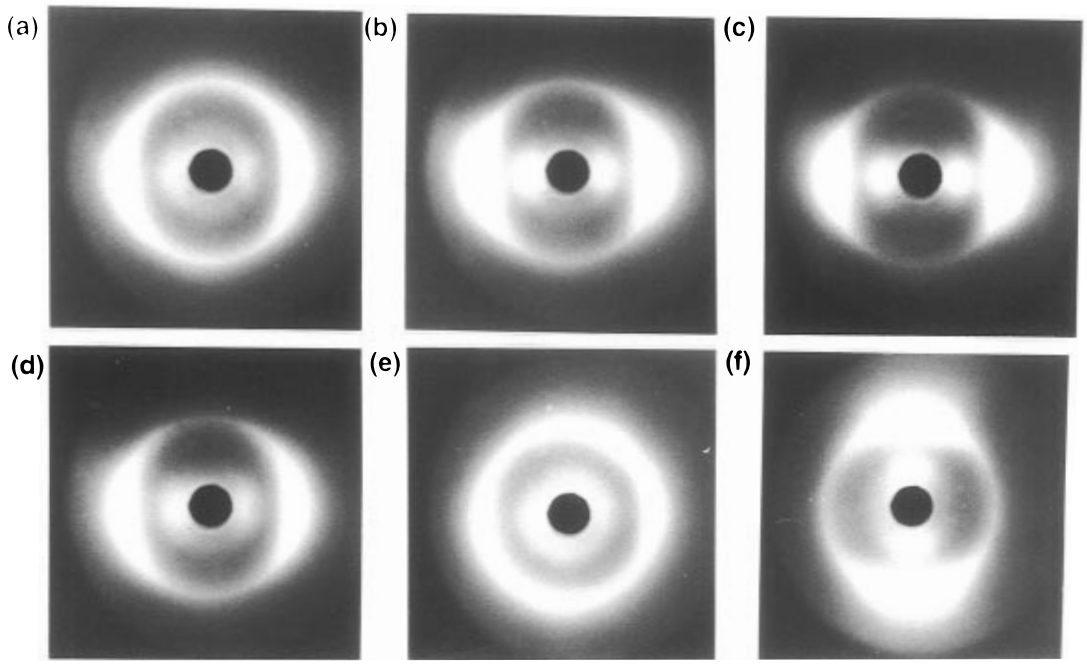

Figure 6. Effect of shear rate $\dot{\gamma}$ on the steady-state flow behavior of B−N 75:25 mol % $\bar{M}_w$ = 8,600 g/mol at 290 °C. *In-situ* transmission wide-angle X-ray diffraction patterns taken at (a) 0.5, (b) 1.0, (c) 5.0, (d) 10, (e) 30, and (f) 60 s^{-1}. In patterns a−d the concentration of equatorial peaks on the velocity axis indicates the orientation of macromolecules along the vorticity axis.

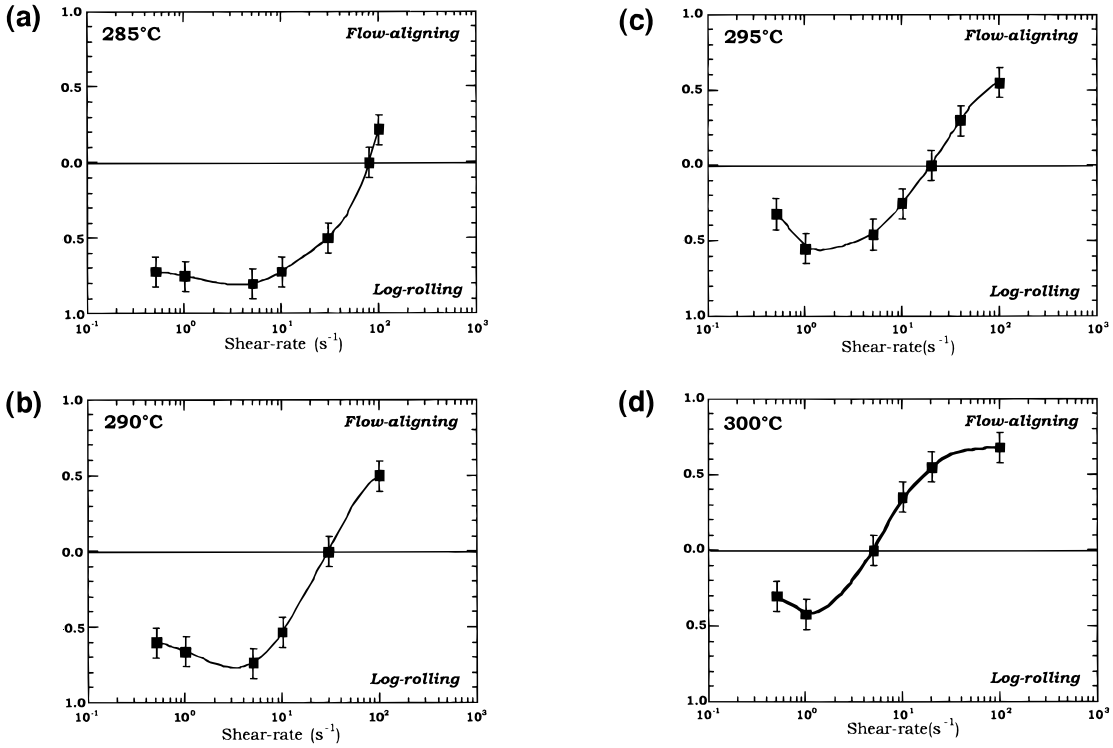

Figure 7. Order parameter $\langle P_2 \rangle$ as a function of shear-rate $\dot{\gamma}$ for log-rolling and flow-aligning regimes for B−N 75:25 mol % $\bar{M}_w$ = 8600 g/mol at (a) 285, (b) 290, (c) 295, (d) and 300 °C. Continuous lines are intended as a guide only.

there is a bimodal orientation distribution with both flow alignment and log-rolling regimes apparent, a feature that can be better appreciated in the contour plot. Further increase in shear rate causes a reduction in intensity of the equatorial peaks on the velocity axis and an increase in those on the vorticity axis.

Transition Parameters. The orientation data are plotted as contours on temperature and strain rate axes in Figure 9, which emphasizes that there is a combination of "critical" shear rate $\dot{\gamma}_c$, and temperature T_c for the transition. Log-rolling occurs in a limited temperature range above the quiescent crystal melting point, the width of this range increasing markedly with decreasing strain rate. The quality of the flow alignment increases with increasing temperature and strain rate, whereas the best log-rolling orientation was achieved at 5 s^{-1}, decaying at higher and lower strain rates and increasing with decreasing temperature.

Samples were quenched from each of the log-rolling and flow-aligning regimes and examined by diffraction along the three orthogonal axes. These results confirmed that the molecular director in each case lay within the plane defined by the velocity and vorticity axes and that the transition between flow alignment and log-rolling corresponds to a reorientation within that plane. These orthogonal patterns for a sample

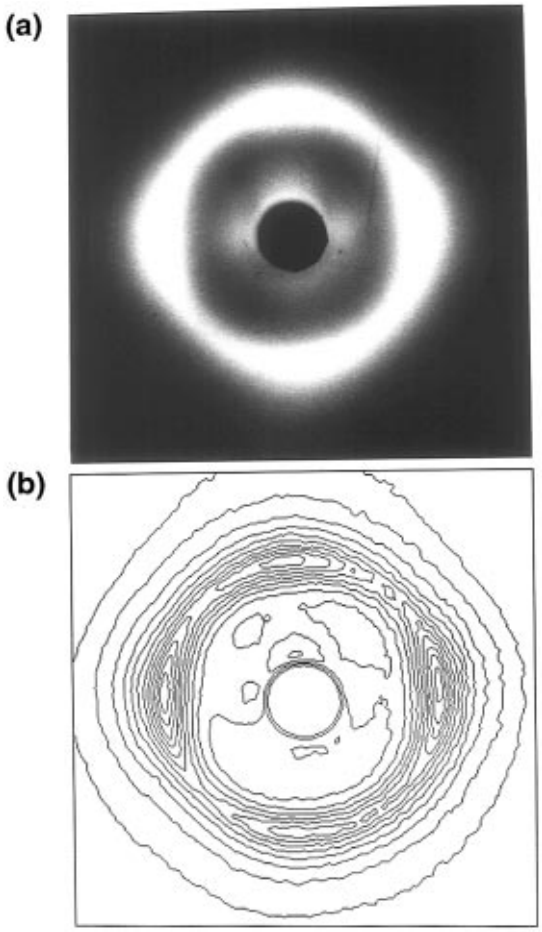

Figure 8. (a) *In-situ* WAXS pattern taken at critical conditions of 295 °C and 15 s^{-1}. (b) Contour plot of pattern shown in (a). Note that this pattern shows the features of bimodal orientation.

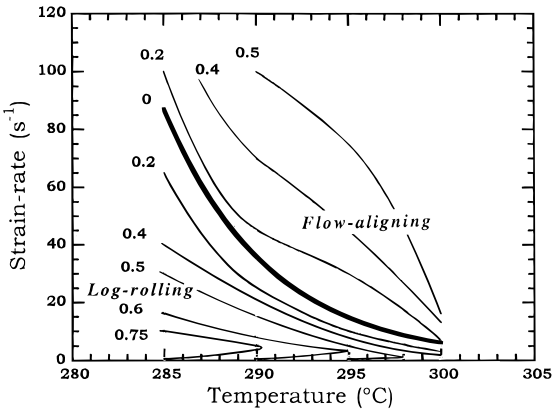

Figure 9. Critical shear rate $\dot{\gamma}_c$ as a function of temperature T. This plot defines the temperature−shear rate parameters for stabilization of either the log-rolling or flow-aligning regime for B−N 75:25 mol % $\bar{M}_w$ = 8600 g/mol. The continuous line corresponds to an exponential fit of the data.

quenched from log-rolling flow are shown in Figure 10a−c. Note that as the specimens are quenched, there is now crystallinity, giving sharper reflections (in 2θ). The pattern 10c obtained with the X-ray beam along the vorticity axis is a uniform ring, which confirms that the orientation has axial symmetry. The corresponding WAXS patterns from a sample quenched from the flow-aligning regime are shown in Figure 11a−c. In this case, the tangential direction (X-ray beam along the velocity axis, pattern 11b) is the one demonstrating the axial symmetry of the alignment.

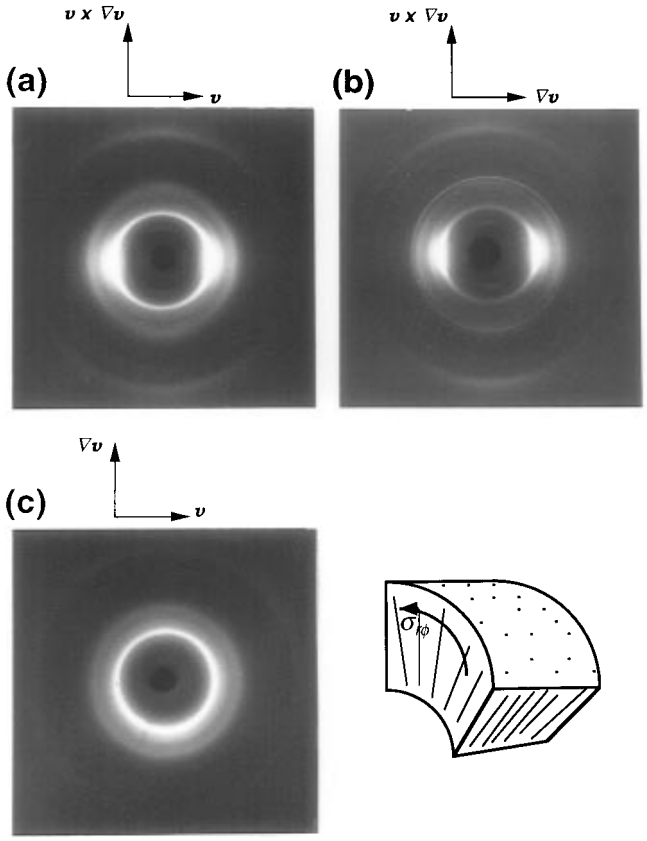

Figure 10. Wide-angle X-ray patterns at room temperature of copolyester cooled while shearing in the log-rolling regime. A pellet was cut from the disk recovered and analyzed along the three-coordinate axis, as indicated in (d). X-ray beam along (a) the velocity gradient axis, (b) the velocity axis, and (c) the vorticity axis. Patterns a and b indicate the preferred alignment of the molecular chains along the vorticity axis, while the unoriented pattern c imaged on the velocity−velocity gradient plane demonstrates that the molecular chains remain on this plane. Cu Kα radiation with graphite monochromator was used.

Reversibility of Transition as a Function of Temperature. It has already been shown that the transition is comparatively invariant under strain rate cycling. At a given temperature, a sample will change orientation from log-rolling to flow alignment and back again with variation in strain rate, within the time resolution of the photographic method (∼10 min). However, the behavior with change in temperature is not as straightforward.

Figure 12 shows the effect of rapidly cooling to 290 °C a sample which had been flow aligned at 315 °C and 10 s^{-1}. In the absence of shear, the flow alignment is maintained at 290 °C, apparently indefinitely, as shown in Figure 12a. The commencement of shearing at rates which would give log-rolling at 290 °C, *viz.*, 5 and 10 s^{-1}, led however to poorly developed orientation even after a period of 30 min, as seen in Figure 12b,c. The log-rolling does not redevelop from the flow alignment when the log-rolling phase field is entered by reducing the temperature. Shear at 30 s^{-1} merely served to reinforce the flow alignment introduced at the higher temperature (Figure 12d). Figure 13 shows azimuthal traces around the main equatorial maximum of the patterns of Figure 12. It is apparent that the weak orientation of Figure 12b−d is actually flow-aligning in nature, despite the conditions of shear.

The results of a different experiment are shown in Figure 14. Here the polymer was sheared at 290 °C and 5 s^{-1} to introduce the log-rolling orientation as in Figure

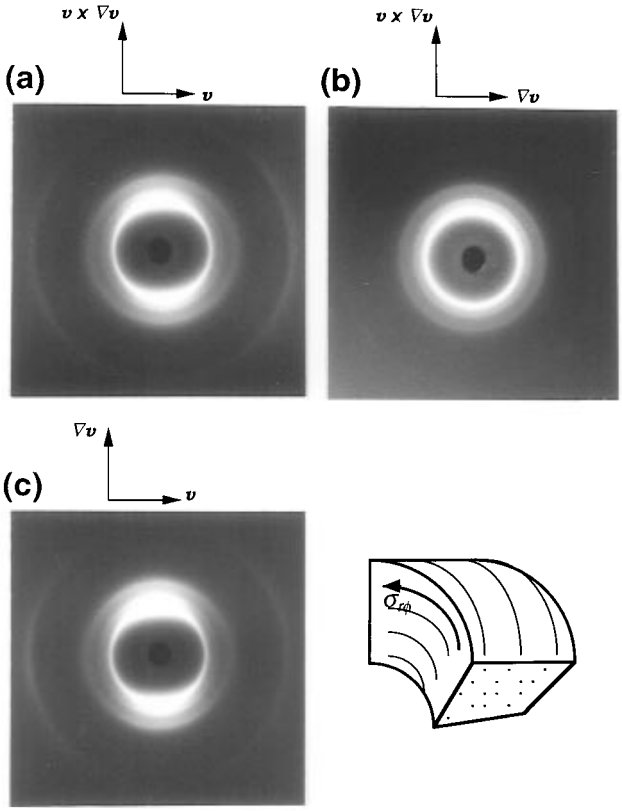

Figure 11. Wide-angle X-ray patterns at room temperature of copolyester cooled while shearing in the flow-aligning regime. A pellet was cut from the disk recovered and analyzed along the three-coordinate axis, as indicated in (d). X-ray beam along (a) the velocity gradient axis, (b) the velocity axis, and (c) the vorticity axis. Patterns a and c indicate the preferred alignment of the molecular chains along the velocity axis, while the unoriented pattern b imaged on the vorticity−velocity gradient plane demonstrates that the molecular chains remain on this plane. Cu Kα radiation with graphite monochromator was used.

14a. The shearing was stopped and the quiescent sample then heated at 20 °C/min to 320 °C and held at that temperature for 1 min before cooling back to 290 °C at the same rate. Immediately on reaching 290 °C, the shearing was recommenced at the same rate. Figure 14b−d shows the redevelopment of the log-rolling regime. Note how the effect of a heating cycle, even without shear, causes the log-rolling orientation to be initially destroyed by the commencement of shear, even though the shear conditions and temperature would put the sample within that regime (*cf.* Figure 8). The fact that it begins to return after longer shearing times is equally eloquent. Figure 15 shows that the same pattern of behavior is observed if the shearing is continued through a high-temperature cycle (320 °C, 1 min) when the orientation would establish as flow alignment. The recovery of the log-rolling regime is gradual, although there is an indication (Figure 15a′,b′) that if the sample is held for a period on return to the low temperature without shearing, then the log-rolling orientation is better developed on recommencement of the 290 °C, 5 s^{-1} shear. By way of contrast, the transition from log-rolling to flow-aligning on heating is as rapid as the strain rate induced transitions.

Effect of Molecular Weight. Investigation of the effect of molecular weight was carried out on specimens with $\bar{M}_w$ = 4600, 5000, 14 400, and 30 000 g/mol, and experiments similar to those described above using material of $\bar{M}_w$ = 8600 were conducted. Shear experiments with the 14 400 and 30 000 g/mol samples did

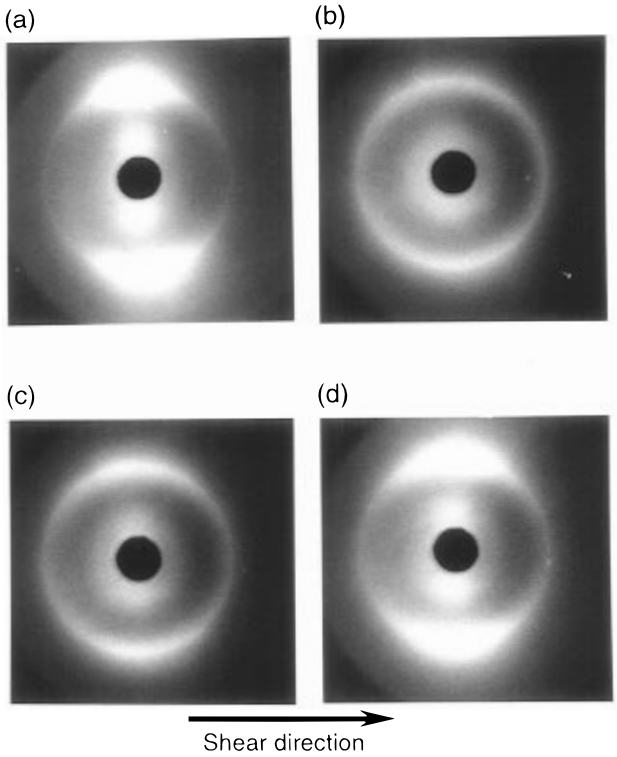

Figure 12. Effect of shear rate $\dot{\gamma}$ on the steady-state flow behavior of B−N 75:25 $\bar{M}_w$ = 8600 g/mol, previously aligned along the velocity axis, at 315 °C and 10 s^{-1}. *In-situ* transmission wide-angle X-ray diffraction patterns taken at (a) 0.0, (b) 0.5, (c) 5.0, and (d) 30 s^{-1}, in each case after 30 min shearing. The flow alignment is compromized at the lower strain rates although the log-rolling regime is not established; $\dot{\gamma}_c$ at 290 °C is 30 s^{-1}.

not give the log-rolling regime, at least over the range of temperatures and shear rates investigated (295−315 °C and 0.5−20 s^{-1}). However, experiments with the samples of 4600 and 5000 g/mol reproduced the series of flow regimes exhibited by the 8600 g/mol polymer. The effect of temperature on the flow dynamics, when shear rate is kept constant, was investigated by taking *in-situ* diffraction patterns between 285 and 315 °C, respectively. Figure 16 shows *in-situ* WAXS patterns corresponding to the 5000 g/mol polymer, taken between 285 and 310 °C, shearing at $\dot{\gamma}$ = 5 s^{-1}. The flow dynamics displayed by the lower molecular weight polymers is in qualitative agreement with that exhibited by the 8600 g/mol polymer, except that the transition to the flow-aligning regime occurs at higher values of shear rate at a given temperature. It is increased from 300 to 305 °C. It might thus be inferred that the temperature/shear rate range for the log-rolling regime increases with decreasing molecular weight and is absent altogether at higher molecular weights, at least at strain rates greater than 0.5 s^{-1}.

Discussion

This paper sets down in detail the observation, first announced as a note,[29] of a strident and reversible orientation transition in a specially synthesized series of thermotropic random copolyester melts of the Vectra A900 type. The transition is between the flow-aligning regime normally seen in nematics and alignment of the global director at right angles to flow alignment and parallel to the vorticity axis, which we refer to as the "log-rolling" regime.

However, the conditions required to achieve log-rolling are quite particular. The regime is observed in

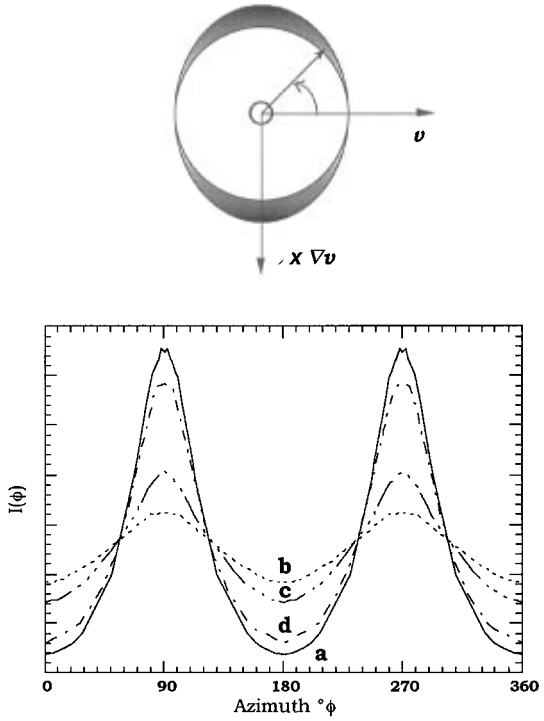

Figure 13. Normalized azimuthal intensity traces through the equatorial peaks of patterns shown in Figure 12 at 290 °C and the following shear rates: (a) 0.0; (b) 0.5; (c) 1.0; (d) 30 s^{-1} . $\phi = 0°$ refers to the velocity (horizontal) axis in the patterns, as indicated schematically. Note that despite the broadening of the equatorials at low shear rates, their maxima remain at 90°ϕ and 270°ϕ, which implies that the director remains aligned along the velocity direction.

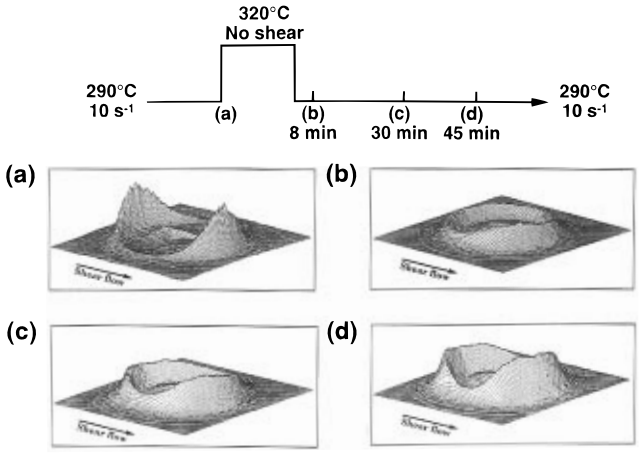

Figure 14. Effect of shear rate on samples that have been cycled in temperature. The *in-situ* WAXS patterns were taken at 290 °C before (a) and after b−d cycling to 310 °C, and the shear rate was kept constant at 5.0 s^{-1}. (a) Before cycling; (b) pattern taken after 8 min; (c) 30 min, and (d) 45 min of continuous shearing. Note that the equatorial peaks gradually reform on the velocity axis showing the gradual re-establishment of log-rolling. The 3D intensity plots are not normalized in order to enhance their features.

a comparatively narrow band of temperature above the crystal melting point, the width of this band decreasing with increasing strain rate and increasing molecular weight. It is possible that above a sufficiently high combination of strain rate and molecular weight, it would not be observed at all above the melting point, although the fact that it is possible to shear these polymers at temperatures below their crystal melting point has not been addressed in this work.

The transition between the log-rolling and flow-aligning regimes is reversible with appropriately varying strain rate and temperature with the caveat that when cooling from flow-aligning to log-rolling, the later regime being only slowly established. Another aspect which must also be noted is that, within a temperature range above the crystal melting point, broadly similar to that in which log-rolling is seen, there is some evidence of flow-induced crystallization, which has also been reported previously.[43] The issue as to whether such crystallization is necessary to drive log-rolling must be faced. Certainly log-rolling is not necessary for this crystallization as it occurs under conditions where flow alignment is the norm. Also, the crystals, which are present in very small amounts, are less perfectly aligned than the molten polymer, and for this reason alone, it is difficult to see how they can be inducing the log-rolling.

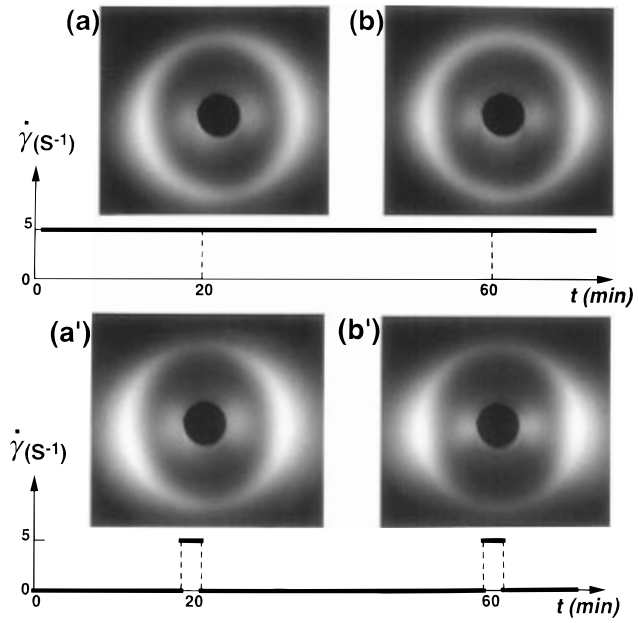

Figure 15. Sequence of experiments similar to those in Figure 14, except that the shearing was maintained during the high-temperature excursion to 320 °C. (a′) and (b′) show the redevelopment of the log-rolling texture after the sample had been held without shearing for periods on returning to 290 °C.

Larson and Öttinger's[28] prediction of log-rolling in nematics may, at first sight, be seen as the basis on which to understand the observations reported. However, while the type of thermotropic polymer studied here is commonly held to be nematic, the log-rolling which is predicted is only metastable. The relationships predicting the rate of change of the three "vector" components of a director

$$\dot{n}_1 = \dot{\gamma} n_2 \left(\frac{\lambda + 1}{2} - \lambda {n_1}^2 \right) \tag{2}$$

$$\dot{n}_2 = \dot{\gamma} n_1 \left(\frac{\lambda - 1}{2} - \lambda {n_2}^2 \right) \tag{3}$$

$$\dot{n}_3 = -\dot{\gamma} \lambda n_1 n_2 n_3 \tag{4}$$

predict that when n_1 and n_2 are zero, that is, if the molecules are aligned along the (log-rolling) vorticity direction, n_3, the three differentials with respect to time will be zero. Hence, a structure which has a log-rolling orientation at start-up should retain that orientation under shear as $\dot{n}_3$ will be zero because n_1 and n_2 are. In contrast, the log-rolling reported here can develop from essentially unoriented textures at start-up, or even as

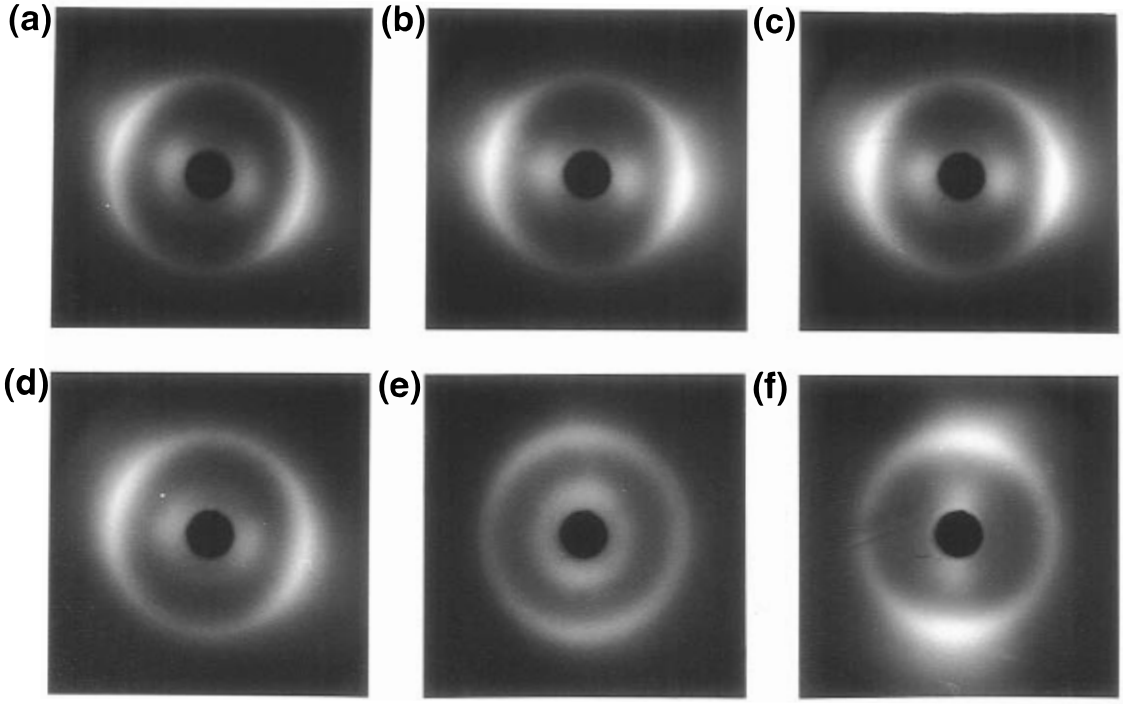

Figure 16. Effect of temperature on the steady-state flow behavior of B−N 75:25 mol % of lower molecular weight, $\bar{M}_w = 5000$ g/mol, while shearing at $\dot{\gamma} = 5\ s^{-1}$. *In-situ* transmission wide-angle X-ray diffraction patterns taken at (a) 285, (b) 290, (c) 295, (d) 300, (e) 305, and (f) 310 °C. In patterns (a−d) the concentration of equatorial peaks on the velocity axis indicates the orientation of the macromolecules along the vorticity axis.

a transition from the flow-aligning state. Furthermore, the nematic theories available do not provide any ready explanation of the confinement of the log-rolling to a relatively narrow temperature band just above the crystal melting point.

Another body of recent work is particularly relevant to this matter. It arose from the consideration of how discrete crystals can form from random copolymer chains such as B−N. The models of localized sequence matching (see ref 42 for example) can explain how crystallinity can develop up to 20% and account for the wide-angle X-ray patterns. While such models are structurally sensible, they run into the difficulty of explaining the observation that the crystals form almost instantaneously on cooling and cannot be prevented by rapid quenching. How then can the matching of adjacent chains produce longitudinal register so quickly? The answer was provided by the measurements of Hanna *et al.*,[14] which showed from X-ray diffraction of aligned melts that the longitudinal register already exists even though there is no evidence for crystallinity. In other words, the melt is smectic-like (smectics in main-chain polymers are better known as "chained smectics" as there is no possibility of slip between the layers[48]), or, more correctly, contains smectic-like domains within a nematic matrix and it is these domains that turn into the crystals. There is thus evidence for smecticity in these polymers, although no measurement so far that would suggest a temperature for the smectic to nematic transition (measurements far above the crystal melting point in these materials are difficult on account of degradation).

The behavior of smectics under shear has been discussed by Krigbaum.[45] Where there is no possibility of shear between the layers, it is observed that the shear direction is normal to the chains (*i.e.*, log-rolling), thus allowing shear deformation without disrupting the layers (Figure 17). One can consider that shear parallel to the chains, which would correspond to flow alignment, is essentially inhibited by a yield stress associated

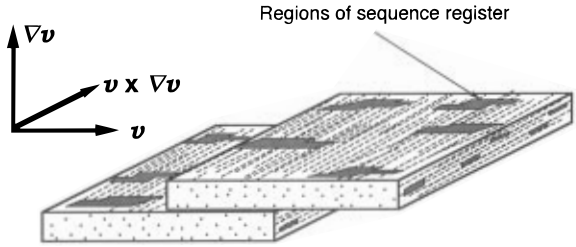

Figure 17. Schematic representation of the flow of nematic B−N copolyester with regions of smectic-type order. The polymer chains run along the vorticity axis. The smectic-type regions correspond to localized matching of sequences of monomer units on the random copolymer chains.[14]

with the integrity of the layers. There is also some evidence that thermotropic polymers, which are smectic by virtue of the segregation of more rigid and less rigid sequences, show a tendency to tumble in the nematic phase in the pretransitional region just above the upper temperature limit of stability of the nematic phase.[44,45] In addition, fairly low molecular weight versions of such polymers have shown orientation orthogonal to the flow direction in both as-spun fibers[45] and quenched samples that had been subjected to oscillatory shear.[46] These two references also indicate that flow alignment, rather than log-rolling, occurred for molecular weights above a particular value.

Another significant issue that should be considered and may add significant insight into the log-rolling flow is that of the molecular weight distribution. It can be suggested that the log-rolling regime would be enhanced as the polydispersity is reduced; *i.e.*, it seems more likely that rods of roughly equal length may be more stable in the log-rolling regime than rods having disparate lengths.

The observation of log-rolling in the main-chain thermotropic random copolymers provides additional confirmatory evidence for the occurrence of a smectic-like phase in isolated regions within a nematic matrix,

which are the precursors of the crystals which form on further cooling.[14] It is possible that the upper temperature limit of the log-rolling provides some indication of a similar limit to the smectic order which has not otherwise been observed. The time taken for log-rolling to reestablish on cooling from temperature excursions well up into the flow-aligning regime is presumably associated with the reestablishment of the smectic-like order.

It is important to face the question of the loss of the log-rolling regime at high molecular weights and higher strain rates. The independent observations of smectic type order[14] gave no evidence of such limitations. We suggest that the low density of entanglements which will occur in liquid crystalline polymers where the chains are less than completely rigid will nevertheless compromise the log-rolling regime as the elements of any random network will always tend to orient with the maximum tensile component of stress. Slow strain rates and lower molecular weights would each tend to enhance the relaxation of entanglements during shear and thus reduce the deleterious effect which entanglements will have on the log-rolling regime. Recent rheological measurements on the same set of polymers add support to this hypothesis.[47]

Conclusions

We have characterized flow-induced orientation transitions in molten thermotropic random copolyesters by using *in-situ* WAXS. Investigation in a range of strain rates, temperatures, and molecular weights have demonstrated that the transition is between the flow-aligning regime normally seen in nematics and alignment of the global director at right angles to flow alignment and parallel to the vorticity axis (out-of-plane orientations), which we refer to as the log-rolling regime. Out-of-plane orientations have been reported in smectic-forming thermotropic polymers with rather low molecular weights. We conclude that regions of local register between chain sequences present in the melt phase, and therefore forming smectic-like regions, are responsible for stabilizing the log-rolling mode in the Vectra A900 type thermotropic copolyesters.

Acknowledgment. We are grateful to Prof. C. Humphreys for laboratory space and Hoechst-Celanese Corp. for the synthesis of special polymer. The advice of Dr. O. Saxton with the image analysis software is gratefully acknowledged, as well as the technical assistance of Mr. B. Seymour in the X-ray laboratory. We thank Dr. S. Hanna, Dr. M. R. Mackley, Prof. G. R. Mitchell, and Dr. J. Odell for useful discussions. A.R.-U. thanks the Mexican Council for Science and Technology (CONACyT-SNI) and the British Council for financial support.

References and Notes

(1) Donald, A. M.; Windle, A. H. *Liquid Crystalline Polymers*; Cambridge University Press: Cambridge, 1992.
(2) Ciferri, A. *Liquid Crystallinity in Polymers: Principles and Fundamental Properties*; VCH: New York, 1991.
(3) Alderman, N. J.; Mackley, M. R. *Faraday Discuss. Chem. Soc.* **1985**, *79*, 149.
(4) Gleeson, J. T.; Larson, R. G.; Mead, D. W.; Kiss, G.; Cladis, P. E. *Liq. Cryst.* **1992**, *11*, 341.
(5) Larson, R. G.; Mead, D. W. *Liq. Cryst.* **1992**, *12*, 751.
(6) Gervat, L.; Mackley, M. R.; Nicholson, T. M.; Windle, A. H. *Philos. Trans. R. Soc. London* **1995**, *A350*, 1.
(7) Larson, R. G.; Doi, M. *J. Rheol.* **1991**, *35*, 539.
(8) Shiwaku, T.; Nakai, A.; Hasegawa, H.; Hashimoto, T. *Macromolecules* **1990**, *23*, 1590.
(9) Almdal, K.; Koppi, K. A.; Bates, F. S.; Mortensen, K. *Macromolecules* **1992**, *25*, 1743.
(10) Picken, S. J.; Aerts, J.; Visser, R.; Northolt, M. G. *Macromolecules* **1990**, *23*, 3849
(11) Straty, G. C.; Hanley, H. J. M.; Glinka, C. J. *J. Stat. Phys.* **1991**, *62*, 1015.
(12) Laun, H. M.; Bung, R.; Hess, S.; Loose, W.; Hess, O.; Hahn, K.; Hädicke, E.; Hingmann, R.; Schmidt, F.; Lindner, P. *J. Rheol.* **1992**, *36*, 743.
(13) Odell, J. A.; Ungar, G.; Feijoo, J. L. *J. Polym. Sci., Polym. Phys. Ed.* **1993**, *31*, 141.
(14) Hanna, S.; Romo-Uribe, A.; Windle, A. H. *Nature* **1993**, *366*, 546.
(15) Keates, P.; Mitchell, G.; Peuvrel-Disdier, E.; Navard, P. *Polymer* **1993**, *34*, 1316.
(16) Okamoto, S.; Saijo, K.; Hashimoto, T. *Macromolecules* **1994**, *27*, 5547.
(17) Balsara, N. P.; Hammouda, B. *Phys. Rev. Lett.* **1994**, *72*, 360.
(18) Kannan, R. M.; Kornfield, J. A. *J. Rheol.* **1994**, *38*, 1127.
(19) Bedford, B. D.; Burghardt, W. R. *J. Rheol.* **1994**, *38*, 1657.
(20) Doi, M. *J. Polym. Sci., Polym. Phys. Ed.* **1981**, *19*, 229.
(21) Marrucci, G.; Maffettone, P. L. *Macromolecules* **1989**, *22*, 4076.
(22) Larson, R. G. *Macromolecules* **1990**, *23*, 3983.
(23) Kiss, G.; Porter, R. S. *J. Polym. Sci., Polym. Symp.* **1978**, *65*, 193.
(24) Navard, P. *J. Polym. Sci., Polym. Phys. Ed.* **1986**, *24*, 435.
(25) Baek, SG.; Magda, J. J.; Larson, R. G. *J. Rheol.* **1993**, *37*, 1201.
(26) Burghardt, W. R.; Fuller, G. G. *Macromolecules* **1991**, *24*, 2546.
(27) Srinivasarao, M.; Berry, G. C. *J. Rheol.* **1991**, *35*, 379.
(28) Larson, R. G.; Öttinger, H. C. *Macromolecules* **1991**, *24*, 6270.
(29) Romo-Uribe, A.; Windle, A. H. *Macromolecules* **1993**, *26*, 7100.
(30) Dadmun, M. D.; Han, C. C. *Macromolecules* **1994**, *27*, 7522.
(31) Penfold, J.; Tiddy, G. J. T.; Staples, E.; Tucker, I. *ISIS Exp. Rep.* **1995**, *RB 6100*, A265.
(32) Richtering, W.; Läuger, J.; Linemann, R. *Langmuir* **1994**, *10*, 4374.
(33) Baek, SG.; Magda, J. J.; Larson, R. G.; Hudson, S. D. *J. Rheol.* **1994**, *38*, 1473.
(34) Giles, D. W.; Denn, M. M. *J. Rheol.* **1994**, *38*, 617.
(35) Kim, S. S.; Han, C. D. *J. Rheol.* **1993**, *37*, 847.
(36) Calunndan, G. W.; Jaffe, M. *The Robert A. Welch Foundation Conferences on Chemical Research, XXVI. Synthetic Polymers*, Houston, Texas, Nov 15−17, 1982.
(37) Krömer, H.; Khun, R.; Pielartzik, H.; Siebke, W.; Eckhardt, V.; Schmidt, M. *Macromolecules* **1991**, *24*, 1950.
(38) Wilson, D. J.; Vonk, C. G.; Windle, A. H. *Polymer* **1993**, *34*, 227.
(39) SEMPER is an image analysis software marketed by Synoptics Ltd.
(40) Cheng, S. Z. D.; Janimak, J. J.; Zhang, A.; Zhou, Z. *Macromolecules* **1989**, *22*, 4240.
(41) Kaito, A.; Kyotani, M.; Nakayama, K. *Macromolecules* **1990**, *23*, 1035.
(42) Hanna, S.; Lemmon, T. J.; Spontak, R. J.; Windle, A. H. *Polymer* **1992**, *33*, 3.
(43) Nicholson, T. M.; Mackley, M. R.; Windle, A. H. *Polymer* **1992**, *33*, 434.
(44) Srinivasarao, M.; Garay, R. O.; Winter, H. H.; Stein, R. S. *Mol. Cryst. Liq. Cryst.* **1992**, *223*, 29.
(45) Krigbaum, W. R.; Watanabe, J. *Polymer* **1983**, *24*, 1299.
(46) Alt, D. J.; Hudson, S. D.; Garay, R. O.; Fujishiro, K. *Macromolecules* **1995**, *28*,1575.
(47) Romo-Uribe, A.; Windle, A. H. *Macromolecules* **1995**, *28*, 7085.
(48) Windle, A. H. In *Liquid Crystalline and Mesomorphic Polymers*, Shibaev, V. P., Lam, L., Eds.; Springer-Verlag: New York, 1994; Chapter 2.
(49) In that paper, the authors used the engineering definition of the shear plane, i.e., the plane normal to the velocity gradient axis, whereas in this paper, the rheological definition of the shear plane is used, i.e., the plane normal to the vorticity axis.

MA960211H